DECISION OF SYSTEM DYNAMICS PARAMETERS IN COMPLEX FLOW PASSAGE THROUGH CFD

Hiroshi HIGO[*], Tomoyuki NAKAMURA[**], Takeshi YAMAGUCHI[***], Kazuhiro TANAKA[****] and Fumio SHIMIZU[****]

[*]Iizuka campus technical support office, Kyushu institute of technology
680-4 Kawazu, Iizuka, Fukuoka, Japan
(E-mail: higo@tech-i.kyutech.ac.jp)
[**]Department of mechanical and control engineering, Tokyo institute of technology
2-12-1, Ookayama, Meguro, Tokyo, Japan
[***]Aisin aw co., LTD
10 Takane, Fujii-cho, Anjo, Aichi, Japan
[****]Department of mechanical information science and technology, Kyushu institute of technology
680-4 Kawazu, Iizuka, Fukuoka, Japan

Abstract. A laminar flow resistance in a pipe is usually used as a representative model of flow resistance because it is convenient to use and often gives reasonable resistance value in a small size pipe under steady state condition. However, the laminar flow resistance model in a pipe is not applicable in an oil flow passage of a real circuit because a flow passage has complex shape in a real circuit. Furthermore, the mathematical model of fluid column in a pipe made in inviscid flow condition is often used as an inertial model in considering dynamic condition. In the real condition of operating oil-hydraulic circuit, the above mentioned two effects, a complex shape of flow passage and flow dynamic characteristics, appears in viscous flow condition. A new model or modeling method to include and solve these effects reasonably becomes necessary. A new modeling method using CFD is introduced in this paper.

Keywords: Oil hydraulic, Oil passage, System dynamics, CFD, Modeling, 1DCAE, Bondgraph

INTRODUCTION

It is important to predict the dynamic characteristics of the whole hydraulic system at the design stage. To predict system dynamic characteristics, the system modeling & simulation method [1-5] is often performed using lumped parameter systems because the calculation load is small and analysis results are provided quickly. The modeling & simulation method needs relevant mathematical equations of all elements corresponding to hydraulic components. Especially, a flow passage which connects hydraulic components and transmits fluid power has a great effect on the system dynamics. Therefore a lot of the studies have been performed [6-7]. Generally, lumped parameter systems of the flow passage can be expressed by resistance, inertia and compressibility, independently. Figure1 shows the representative full model of flow passages using Bondgraph method. C-element is connected to 0-junction and I-element and R-element are connected to 1-junction, respectively. So far, the equivalent Eq. (1) - (3) have been used as the mathematical models of flow passage [8-10]. The Eq. (1), (2) and (3) shows resistance effect, inertial effect of fluid column in the flow passage and fluid compressibility (capacitance) effect, respectively. These equations are derived as the lumped parameter models with regarding straight pipe. However, the actual hydraulic device has flow passages with very complex shape and the working oil flows three-dimensionally with strong nonlinearity. In case of the complex flow passage, these conventional equations cannot be applied exactly.

Resistance R-element $$\Delta P = \frac{128\mu L}{\pi D^4} Q_2 \quad (1)$$

Inertia I -*element* $$Q_2 = \frac{A}{\rho L}\int (P_1 - P_2 - \Delta P)dt \quad (2)$$

Capacitance C-element $$P_1 = \frac{K}{V}\int (Q_1 - Q_2)dt \quad (3)$$

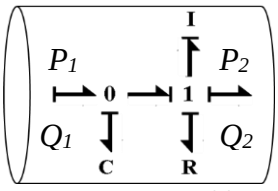

FIGURE 1. Bondgraph model of flow passage

On the other hand, computer technology has been developed and numerical precision of Computational Fluid Dynamics (CFD) has been improved in recent years. Many studies of flow passage using CFD have been performed widely.

The first purpose of this study is to propose how to make highly precision models of flow passages with any complex shape, and then to investigate accuracy of the proposed modeling method by applying to a piping system with orifice. Furthermore, the dynamic characteristics of a complex flow passage are studied as combination of basic pipe elements through inspection of the calculation precision.

NEW MODELING METHOD

As the Eq. (3) is expressed by volume and bulk modulus of fluid elasticity only, the shape of flow passage does not influence compressibility of the flow fluid. Thus, in this study, compressibility can be calculated by considering only the volume of flow passage.

On the other hand, according to Eq. (1) and Eq. (2), resistance and inertia are influenced by flow condition which caused by shape of flow passage obviously. The resistance and inertia effects are examined from this. Eq. (4) indicates that resistance of flow passages which have any shape can be expressed by non-linear and linear terms.

$$\Delta P = RQ + R'Q^2 \tag{4}$$

$$Q = \frac{1}{I}\int (P - \Delta P)dt \tag{5}$$

The 1st term indicates a laminar flow resistance and 2nd term, an orifice/restriction resistance, respectively. And then from Newton's the second law without flow friction, inertia of fluid column in the flow passage is expressed by Eq. (5). By defining these characteristic equations, the flow passage with any shape will be able to be defined by the properties of flow passage universally. The traditional inertial element and resistance element are often defined independently. However these effects are linked each other [11]. Therefore, it is necessary to decide the parameters to satisfy these elements simultaneously. In this study, a new model for satisfying each elements simultaneously (Simultaneous Inertia-Resistance model: here after, SIR model) will be proposed.

Resistance Characteristic in Eq. (4)

The characteristic of resistance is expressed by the relationship between pressure and volume flow rate. Generally, the graph is called as a ΔP-Q diagram. Unsteady pressure loss is ignored in this study, thus the resistance model is assumed to be calculated under quasi-steady state condition. The ΔP-Q diagram is obtained by CFD steady flow analysis which is performed on the condition that the inlet boundary setting is given as flow rate and outlet boundary setting is given as pressure. The pressure loss in the flow passage is calculated as the pressure difference between the inlet and the outlet. By repeating this calculation process, the ΔP-Q diagram between the flow rate and the pressure drop is obtained. The coefficients of the resistance parameter, R and R' are derived from calculation results in ΔP-Q-diagram by least squares approximation. By the above numerical method, the mathematical model with the non-linear flow resistance in a flow passage can be derived.

Inertia Characteristic in Eq. (5)

Eq. (6) which expresses dynamics of flow passage is obtained by substitution Eq. (4) for Eq. (5).

$$I\frac{dQ}{dt} + RQ + R'Q^2 = P \tag{6}$$

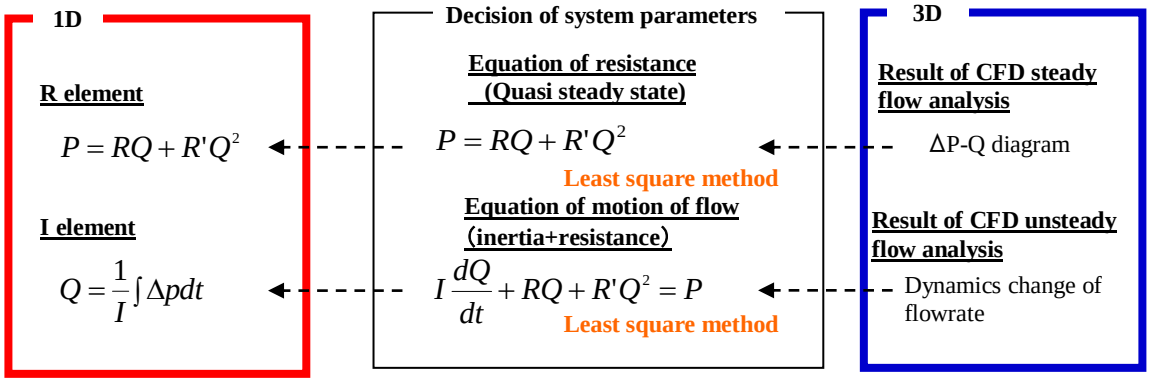

FIGURE 2. Derivation of characteristic parameters such as R, R' and I

To derive the characteristic of fluid inertia *I*, the time change of the flow rate (dynamic change of flowrate) is calculated by performing CFD unsteady flow analysis when the steady state becomes the transient state by giving a step-formed pressure input. In this case, the pressures are given as the inlet and outlet boundary conditions. The solution of Eq. (6) consists of the parameters such as *I, t, P, R* and *R'*. The inertial characteristic *I* is calculated by applying a least squares approximation method to the dynamic change of the calculated flow rate, Q. A flow chart of decision of coefficient *R, R', I* using CFD results is shown in Figure 2.

VALIDATION OF SIR MODEL

Straight Pipe

The SIR model applied to a straight pipe and the effects by pipe diameter and length are investigated. The diameters of the pipe is 2[mm] and 4[mm], and the length is 50-800[mm]. Table 1 shows the numerical calculation conditions and the shape parameters for these calculations are shown in Fig. 3.

TABLE 1. Calculation conditions of simple pipes

Calculation Parameters	
Diameter of pipe [mm]	2, 4
Length of pipe [mm]	50, 100, 200, 300, 400, 800
Boundary condition	
Inlet	$1\times10^{-6} \sim 1\times10^{-5}$ [m^3/s]
Outlet	0 [Pa]
Calculation condition	
Property of fluid	ρ =853 [kg/m^3] μ =0.0302 [Pa·s]
Number of mesh	300,000 Tetra

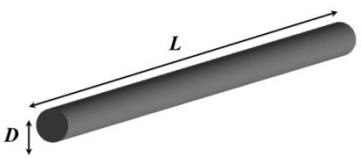

FIGURE 3. Calculation target

Results

The mathematical model of the resistance of straight pipe in case of laminar flow is expressed by Eq. (1) and then the parameter of resistance is expressed by Eq. (7).

$$R_{sp} = \frac{128\mu L}{\pi D^4} \tag{7}$$

Figure 4 shows the comparison of the results by conventional model with them by SIR model. From this figure, it is found that the results agree well, each other.

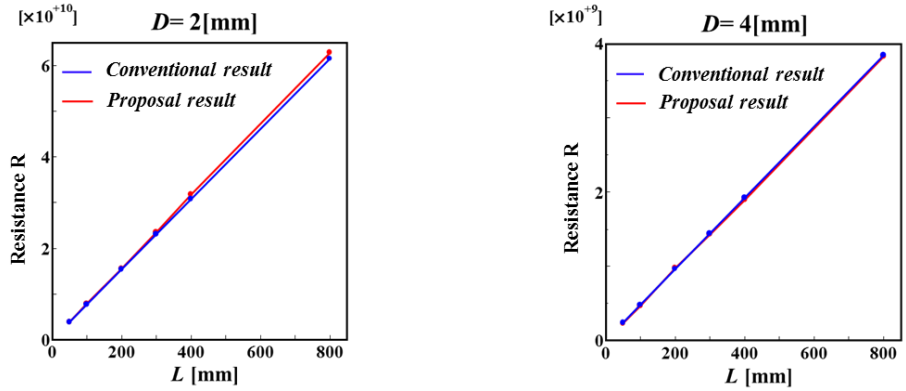

FIGURE 4. Comparison of resistance characteristic between conventional model and SIR model

Conventionally, inertia of straight pipe is calculated from acceleration of fluid column in control volume which acts on pressure difference of control volume in the assumption of inviscid flow. The inertia parameter *I*, which is derived from Eq. (2) is expressed by Eq. (8). The comparison of the inertia parameter of conventional model with SIR model is shown in Fig. 5.

$$I_{sp} = \frac{\rho L}{A} \tag{8}$$

As can be seen from this figure, these results of Inertance *I* parameters do not agree and coefficient *I* of SIR model is 1.3 greater than that of conventional model. For the reason, *I* of Eq. (8) is derived from inviscid flow assumption and *I* of SIR model is derived to satisfy resistance and inertia simultaneously, based on CFD results

which assumes to viscous flow. It is thought that SIR model can calculate more correctly than the conventional model.

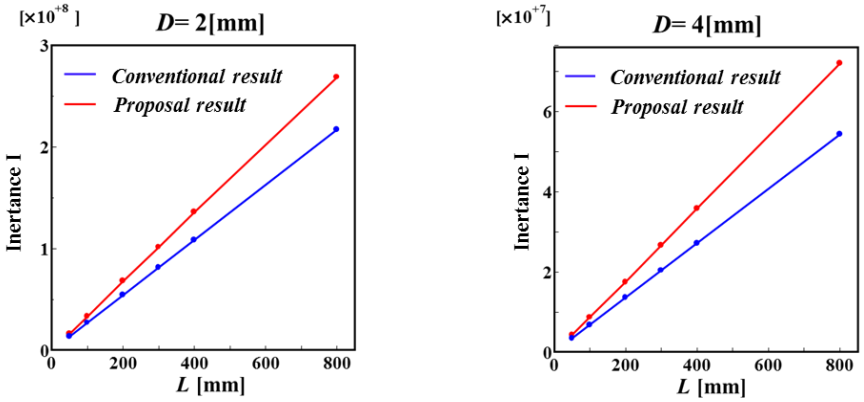

FIGURE 5. Comparison of inertia characteristic between conventional model and SIR model

TABLE 2. Calculation conditions of orifice pipe

Calculation Parameters	
Diameter of pipe [mm]	4
Length of pipe [mm]	100, 200, 300, 400
Diameter of orifice [mm]	0.6, 0.8, 1.0
Length of orifice [mm]	1.0
Boundary condition	
Inlet	1×10^{-6} ~ 1×10^{-5} [m^3/s]
Outlet	0 [Pa]
Calculation condition	
Property of fluid	ρ =853 [kg/m^3] μ =0.0302 [Pa·s]
Number of mesh	450,000 Tetra

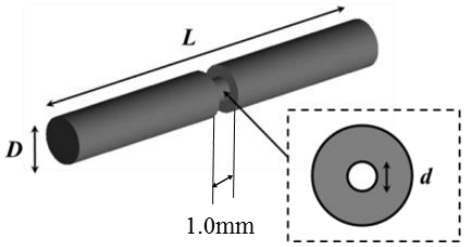

FIGURE 6. Calculation target

Orifice Pipe

Next, SIR model is applied to an orifice pipe. Figure 6 and Table 2 show analysis target and calculation conditions, respectively.

Results

In this case, pressure loss can be expressed by Eq. (9). Traditionally the flow coefficient c is 0.7.

$$P_{ori} = \frac{\rho}{2c^2 A_{ori}{}^2} Q^2 \tag{9}$$

Thus, mathematical model of resistance for orifice pipe could be considered to sum of Eq. (7) and Eq. (9), eventually it can be expressed by Eq. (10).

Figure 7 illustrates the ΔP-Q diagram obtained from Eq. (10) and from SIR model. As shown in this figure, the pressure losses obtained by the both models agree well in all case of different diameter of orifice. Figure 8 and 9 indicate that the relationship between resistance parameter R, R' and length of orifice pipe.

$$P = \frac{128\mu L}{\pi D^4} Q + \frac{\rho}{2c^2 A_{ori}{}^2} Q^2 \tag{10}$$

It is found that parameters R and R' become higher as the orifice diameter decreases. Although R' is independent of pipe length, R increases at linear function of pipe length. The reason for this, the parameter R expresses resistance of straight pipe in case of laminar flow. Furthermore, pressure loss is shown to be a square function of volume flow rate due to orifice.

Thereupon, the effect of loss is investigated about this calculation. For example, the breakdown of the total pressure loss at the orifice diameter 1.0[mm], pipe length 400[mm] is investigated. The influence of orifice is the smallest in these calculations. In this case, it is found that R is 3.55×10^9[$kg/(m^4s)$], R' is 1.33×10^{15}[kg/m^7]. Hence, 1st term of Eq. (9) is 35.5[kPa], whereas 2nd term is 133.0[kPa]. Thus, it is found that the effect of orifice is greater than length of pipe.

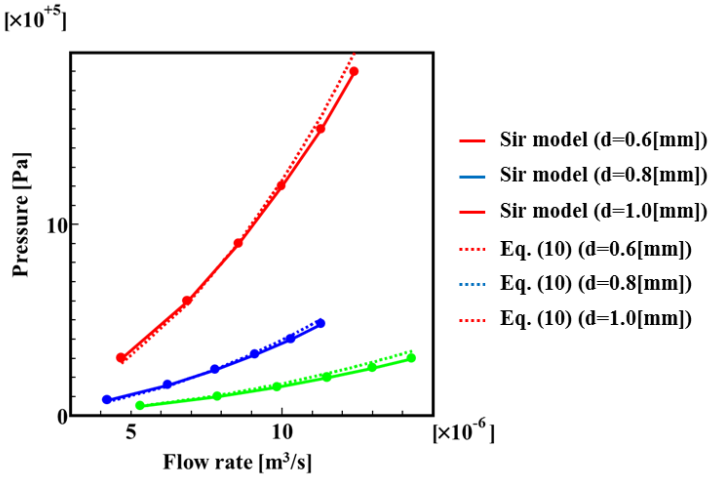

FIGURE 7. Comparison of ΔP-Q diagram between conventional model and SIR model

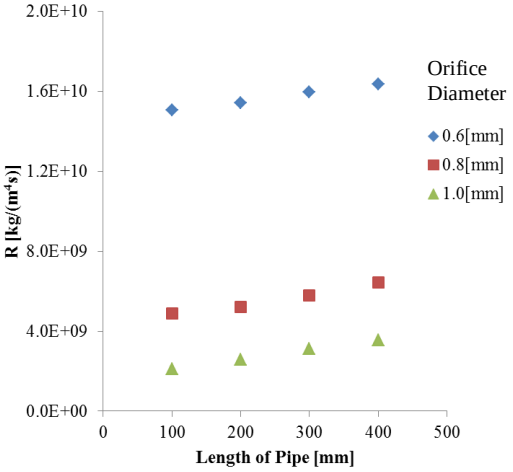

FIGURE 8. Relationship between *R* and pipe length

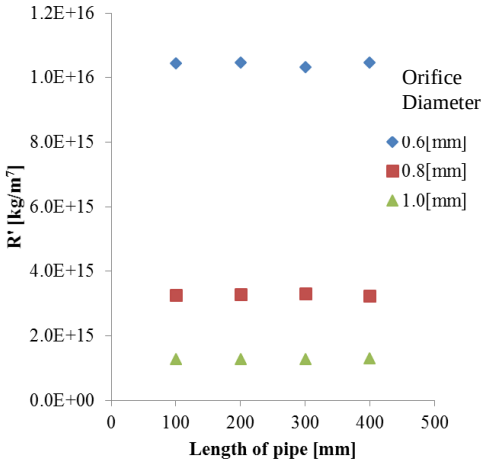

FIGURE 9. Relationship between *R'* and pipe length

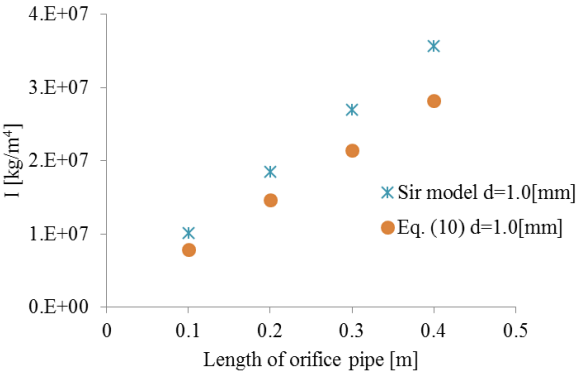

FIGURE 10. Relationship between *I* and orifice pipe length

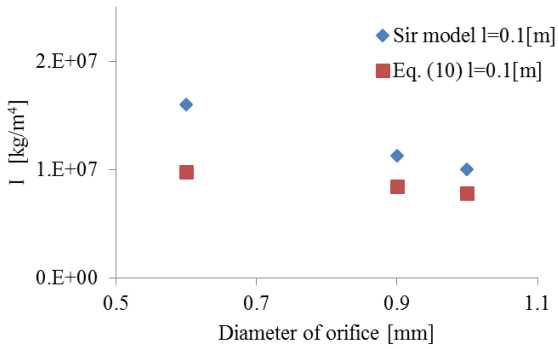

FIGURE 11. Relationship between *I* and orifice diameter

On the other hand, the mathematical model of inertia for orifice pipe is sum of the inertia parameter *I* for a straight pipe and for an orifice, as follows[7].

$$I_{op} = \frac{\rho L_{pipe}}{A_{pipe}} + \frac{\rho L_{ori}}{A_{ori}} \tag{11}$$

Eq. (8) can use for each element, and then Eq. (11) can be derived. Figure 10 shows a comparison between the inertia parameter by Eq. (10) and by SIR model.

Figure 10 shows the relationship between inertia parameter I and length of orifice pipe. The length is shown to be a linear function of inertia parameter *I* similarly with conventional model and SIR model. However, the inertia parameter *I* differs each other. It seems that the effect of orifice cannot be estimated correctly by the

conventional model in Eq. (11). Figure 11 shows the relationship between orifice diameter and the inertia parameter *I*. The orifice diameter decreases with increasing inertia parameter *I*. And difference of conventional model and SIR model increases, gradually.

Figure 12 shows flow rate changes over time in the flow passage when pressure inputs are given as step function. Table3 shows the numerical errors of steady flow rate and the time constant with respect to the CFD results. It is indicated that the error on steady volume flow rate and time constant of the conventional model are 2.7[%] and 18.1[%] compared with 3D-CFD model, respectively. This error causes the flow condition as inviscid/viscous flow. SIR model is based on CFD results, and then the error becomes smaller than the conventional model.

Figure 13 illustrates streamline of the orifice pipe using CFD. The vortex that occurs near the orifice exit grows up with time, and it is revealed that it becomes steady flow in approximately 4[msec]. Therefore, the inertial effect becomes active and important in very short time.

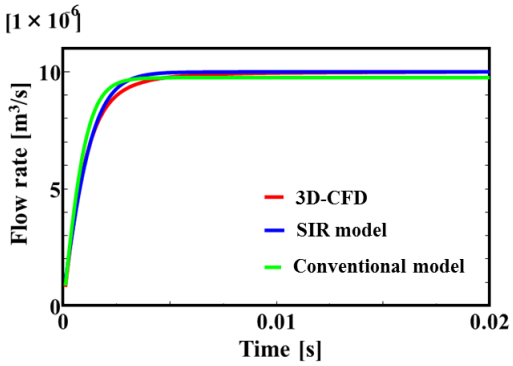

FIGURE 12. Dynamic changes of flowrate

TABLE 3. Comparison of numerical error between conventional model and SIR model

Modeling method	Error of steady flowrate	Error of time constant
SIR model	0.2 [%]	9.1 [%]
Conventional model	2.7 [%]	18.1 [%]

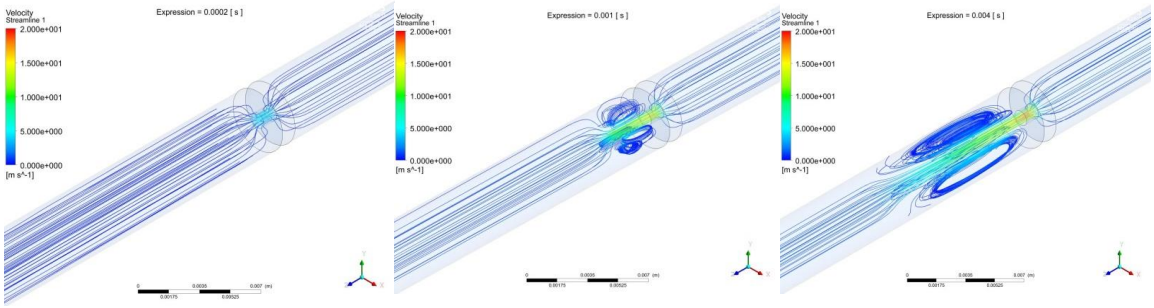

0.2[msec] 1[msec] 4[msec]

FIGURE 13. Stream line of orifice pipe

COMBINATION OF SYSTEM PARAMETERS

In general, the flow passage consists of several basic piping units with various shapes. In this chapter, it will be confirmed that the parameter of whole piping system can be calculated by combination of each piping unit parameter. The total pressure loss ΔP_{all} of pipes be calculated by sum of each partial pressure loss ΔP_n. (Eq. (12))

$$\Delta P_{all} = \Delta P_1 + \Delta P_1 + \cdots + \Delta P_n \tag{12}$$

Because the flow rate Q of each flow passage is the same, Eq. (13) is derived.

$$\Delta P_{all} = \left(\sum R_i\right)Q + \left(\sum R_i'\right)Q^2 \tag{13}$$

Therefore, each coefficient of the resistance parameters of a connected flow passage can be calculated by sum of the respective coefficients of the resistance parameters, R_i and R_i' .The inertial characteristic of the flow

passage consisting of the n units is represented by Eq. (14). As a result, the inertial characteristics of connected flow passage is calculated by sum of partial inertial effects, as shown in Eq. (15).

$$I_1 \frac{dQ}{dt} + I_2 \frac{dQ}{dt} + \cdots + I_n \frac{dQ}{dt} = P - \Delta P_1 - \Delta P_2 - \cdots - \Delta P_n \tag{14}$$

$$\left(\sum I_n\right)\frac{dQ}{dt} = P - \Delta P_{all} \tag{15}$$

Calculation Condition

Figure 14 shows an analysis model to inspect the connection of the partial parameters shown in Figure 14(a) straight pipe, (b) orifice pipe and (c) curve pipe.

The system parameter calculated as each SIR model on the three kinds (a), (b) and (c) are summed up as a connected pipe according to Eq. (11) and Eq. (15). And for a check, the system parameters are compared with the CFD results on the (d) model. Figure 15 shows the tetra mesh used in this calculation.

Results

Figure 16 shows the comparison of the results summed up system parameters of such SIR model as A, B and C, shown in Figure14, with 3D-CFD results calculated on D as one whole model. Figure 16(a) and (b) shows the ΔP-Q diagram and time change of the volume flow rate, respectively. These results agree well in the both figures, approximately. It shows the fact that the dynamic system parameters of a connected pipe can be obtained as a whole system by summing up the partial system parameter of each SIR model.

Then, the numerical precision is studied. Table 4 shows the system parameters as SIR model of three kinds of piping element, A, B and C. The whole pipe model D consists of one straight pipe A, two orifice pipes B and two curved pipes C, which is expressed as the pipe (A+2B+2C).

The system parameters are compared between the connected pipe (A+2B+2C) and the whole pipe D in Table 5. Top line of Table 5 shows the parameters, such as *I*, *R* and *R'*, of the pipe (A+2B+2C) which are calculated by sum of the partial parameters of each basic pipe A, B and C. And second line shows the result calculated in D as one whole model by 3D-CFD. As a result, it is found that this technique can calculate the system dynamic parameters with less than 7% errors. It is considered that the errors are caused by the applying precision of a least squares approximation and the difference of the velocity profile in the boundary surface between the connected pipes. Finally, it was verified that the SIR model gives dynamic system parameters of each piping element reasonably and the dynamic parameters of a whole system can be obtained by summing up the partial system parameter of each SIR model.

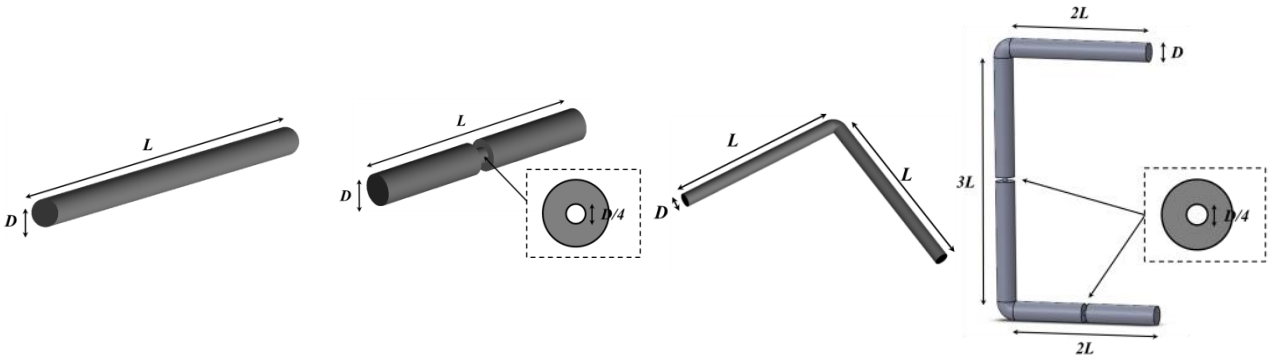

(a) Straight pipe; model A (b) Orifice pipe; model B (c) Bend pipe; model C (d) Connected pipe; model D

FIGURE 14. Models for the simulation

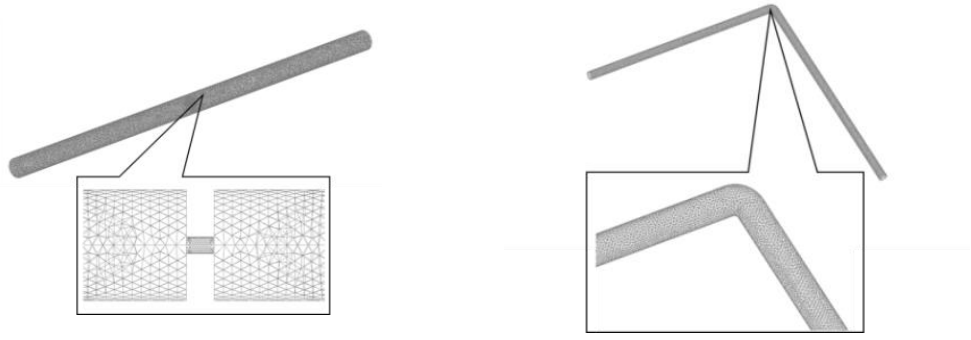

FIGURE 15. Numerical grids

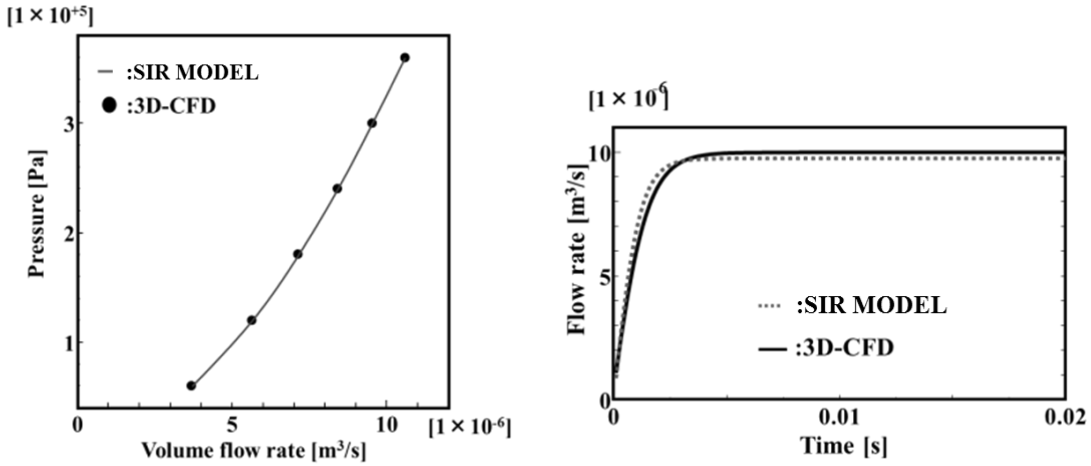

(a) PQ diagram (b) Flow rate (unsteady)

FIGURE 16. Graph for decision of parameters on combination pipe

TABLE 4. System parameters of the pipes

Pipe type	*I*	*R*	*R'*
A: Straight	8.71×10^{6}	4.64×10^{8}	6.54×10^{12}
B: Orifice	1.02×10^{7}	2.31×10^{9}	1.32×10^{15}
C: Bend	1.78×10^{7}	9.58×10^{8}	1.15×10^{13}

TABLE 5. Comparison of system parameters

Method	*I*	*R*	*R'*
A+2B+2C	6.48×10^{7}	7.00×10^{9}	2.67×10^{15}
Connected	6.23×10^{7}	6.55×10^{9}	2.61×10^{15}
Error [%]	4.0	6.9	2.5

CONCLUSION

In this paper, a new method to decide system dynamic parameters of pipes with any complex shape based on lumped parameter system is introduced using CFD analysis. The new modeling method, SIR model, which can satisfy real resistance and inertia simultaneously in a flow passages with any shape is validated by comparing the CFD results in a straight pipe and orifice pipe. It is found that the resistance of SIR model is almost equal to a conventional model using laminar flow resistance as well as orifice model.

Furthermore, inertia effect of SIR model becomes useful in a real condition because it is based on CFD analysis needless to say, different from conventional mathematical model of fluid column, which is made in a pipe in inviscid flow condition.

The new model, SIR model, gives numerically precise dynamic system parameters of each piping element and the dynamic parameters of a whole system can be obtained by summing up the partial system parameter of each SIR model.

REFERENCES

1. Rosenberg R.C. and Karnopp D.C., Introduction to Physical System Dynamics, McGraw-Hill1983.
2. Thoma J., Simulation by Bondgraphs, Springer-Verlag, 1990.
3. Rosenberg R.C.,Reflection of Engineering system and Bondgraphs, Journal of dynamic systems, measurement, and control, vol.115, 1993, pp. 242-251.
4. Sakurai Y., Tanaka K., Kohda T., and Nakada T., Connection of Bondgraph Model and Basic Structure of Oil-hydraulic Component icon in OHC-SIM, IECON2000, 2000, pp. 1562-1567.
5. Amalendu Mukherjee, Ranjit Karmakar, Modelling and Simulation of Engineering Systems through Bondgraphs, CRC Press, 2000
6. Higo H., Yamamoto K., Tanaka K., Sakurai Y., and Nakada T., Bondgraph Analysis on Pressure Fluctuation in Hydraulic Pipes, IECON2000, 2000, pp. 1556-1561.
7. Pozrikids C. K., Fluid Dynamics Theory, Computation and Numerical Simulation, Academic Publishers, 2001, pp. 308.
8. Gary Z Watters, Analysis and Control of Unsteady Flow in pipeline, Butterworth Publishers, 1984, Chap. 2.
9. Benjamin E. W., Victor L.S., Fluid Transient in Systems, PRENTICE HALL, 1993, pp. 2-9.
10. Higo H., Tanaka K., Yamaguchi T., New One Dimensional Modeling for Complex Oil Passage Coupled with CFD Results, Proceedings of the ASME/BATH 2014 Symposium on Fluid Power & Motion Control FPMC2015, 2014.
11. D. Nigel Johnston, Prediction of Fluid Inertance in Nonuniform Passageways, Journal of Fluids Engineering 128(2), 2006.

